Hydrodynamic and sediment transport characteristics of an offshore wind farms in complex hydrodynamic environments

Jing Wang[a,b], Liangwen Jia*[a,b]
[a]School of Ocean Engineering and Technology, Sun Yat-sen University, Zhuhai 519082, China;
[b]Southern Marine Science and Engineering Guangdong Laboratory (Zhuhai), Zhuhai 519082, China
*Corresponding author email: jialw@mail.sysu.edu.cn

ABSTRACT

This study analyzes the Guishan Offshore Wind Farm in the Lingdingyang Estuary. In situ observations and a three-dimensional numerical model were used. The results show that the wind farm alters the regional flow field and suspended sediment transport. The response varies with foundation type and location. Flow acceleration mainly occurs within the channels between foundations. Flow reduction is more common in foundation wakes and along the outer boundary of the array. Local velocity differences can reach 0.5 m/s. Changes in suspended sediment concentration (SSC) are mainly concentrated near the seabed. The response decreases from the bottom layer to the surface layer. Most suspended sediment concentration differences are on the order of 10^{-3} and 10^{-2} kg/m^3. These findings suggest that wind farm disturbances can further influence near-bed sediment resuspension and particle settling processes by modifying the local flow structure, thereby leading to a redistribution of the regional suspended sediment field.

Keywords: Offshore wind farm; flow structure; suspended sediment concentration; complex hydrodynamic environment; coupled hydrodynamic-sediment model

1. INTRODUCTION

The vertical structures of offshore wind turbine foundations, spanning the entire water column, exert significant disturbances on the surrounding flow field. For a monopile foundation, the incoming flow is obstructed, leading to a backwater effect on the upstream side and the formation of a wake zone downstream [1-3]. When the scope of study expands from a single pile to an array or a full-scale wind farm, the superposition and interaction of individual wakes further modify the dynamic transport structure at both local and regional scales [4-6]. With the continuous expansion of offshore wind energy, array-scale hydrodynamic effects have received increasing attention[7-9]. Several methods have been used to identify regional changes caused by wind farm clusters. Christiansen and Hasager [10] used synthetic aperture radar (SAR) observations to detect clear wake patterns downstream of offshore wind farm. Their results indicated that flow disturbances can extend over kilometer scales. Other scholars have combined computer models with satellite data, and have come to the same conclusion, that the tidal change in the offshore wind farm is relatively small, about 5% to 10% [11]. Hosseini et al.[12] said that the change of wave can reach 20 kilometers, which means that the offshore wind farm will not only be affected by the surrounding foundation, but also cause water movement in the wind farm area.The construction of wind turbine foundations will lead to changes in water flow, which will lead to changes in sediment movement.The suspended sediment will spread in the water, the sediment on the seabed will move, and the Landsat-8 satellite can detect turbid water in the downstream area[13], which can reach several kilometers, with a width of 150m to 30m.Sentinel-2 data show that the suspended particle concentration in the water is 10% to 20% lower than that in the surrounding water[14]. The plume direction also changed with the tidal phase. Coupled numerical modeling further linked these patterns to changes in local velocity and bed shear stress [15].

Previous studies have mainly examined wake dynamics around individual foundations. However, the regional responses of flow and suspended sediment concentration remain less understood. Estuarine processes are strongly affected by tides, topography, and sediment conditions. Therefore, array-scale effects cannot be inferred directly from single-foundation studies. This study uses the Guishan Offshore Wind Farm in the Lingdingyang Estuary as a case study. It examines the spatial changes in regional currents and suspended sediment transport caused by the presence of the wind farm. By comparing changes under realistic tidal and wave conditions, we aim to identify which key processes drive this large-scale hydrodynamic reorganization.

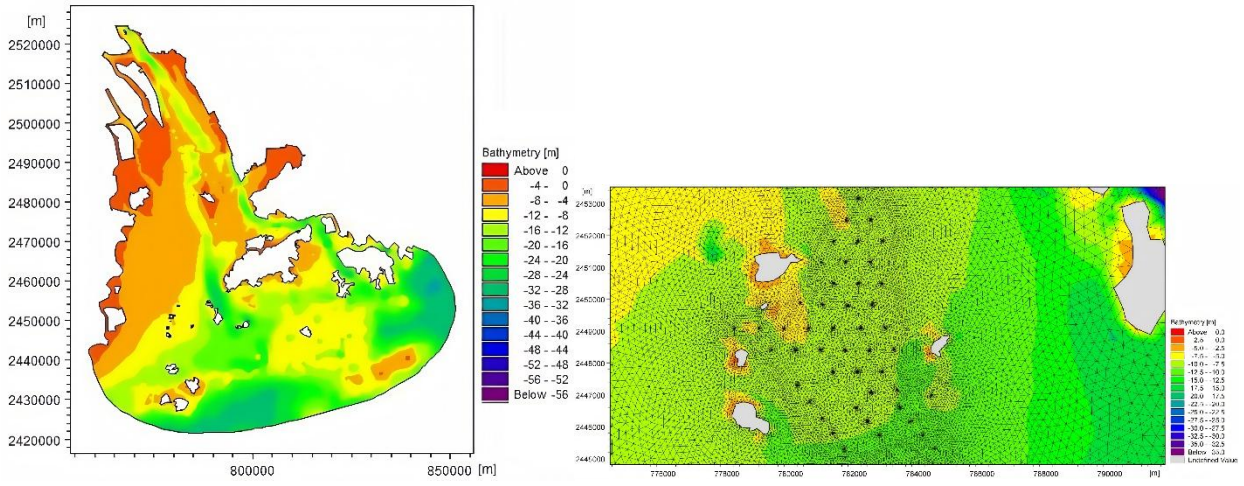
International Conference on Advances in Energy and Environmental Engineering (AEEE 2026), edited by Najib Essounbouli, Guang-Liang Feng, Hamid Gualous, Proc. of SPIE Vol. 14510, 1451007 · © The Authors. Published under a Creative Commons Attribution CC-BY 4.0 License · doi: 10.1117/12.3124761

2. STUDY AREA

The Guishan Wind Farm is located in the southern Lingdingyang Estuar. The water depth is about 10 m, with some locations reaching 20–30 m. Because of the Pearl River runoff, tides, and waves, it exhibits the complex characteristics typical of an estuary-coastal zone. The Pearl River's annual average runoff is 3457.8×10^8 m³, or about 10,000 m³/s on average. The tides are of the irregular semi-diurnal type. The flood and ebb currents veer toward the eastern and western sides, respectively. The wind farm is exposed to open water. Waves come mainly from the east 34% of the time, with an average height of 1.4 m and a recorded maximum of 4.9 m. Surface sediments are mostly silts and sands. In the core area, mean grain size is 5–7 φ.

3. MODEL SETUP AND VALIDATION

The study area is the Guishan Offshore Wind Farm in the LE. The UTM coordinate system and the Pearl River Vertical Datum are used here. The study boundary are set at the four upstream river mouths: Humen, Jiaomen, Hongqili, and Hengmen. The seaward boundaries are the coastal waters near Coloane Island, Dawanshan Island, and Tseung Kwan O. The mesh has 35,898 nodes and 69,120 triangular elements. It uses the unstructured and non-uniform grid. Moreover, it can achieve high resolution while keeping the computational cost under control. Near the foundations of the wind turbine, the grid will be locally refined. The minimum grid size is 2 m near monopiles and 0.5 m near jacket piles. In contrast, the grid scales at the land and open-sea boundaries range from 200-500 m and 1,000 m, respectively. The model mesh configuration is illustrated in Figure 1.



(a) (b)

Figure 1. Study area model and grid configuration: (a) scope and water depth of the study area; (b) Local grid meshing of the wind farm.

The model calibration period is from December 27, 2019, to January 5, 2020. Upstream boundaries were driven by field observations, while the open-sea boundary utilized TPXO tidal predictions. The sediment bed consists of three layers, with a median grain size of 0.04 mm, a settling velocity of 0.0002 m/s, and a critical shear stress for deposition of 0.1 N/m^2. The thicknesses of the three layers were 0.2 m, 0.3 m, and 0.3 m, respectively. The corresponding erosion coefficients are 2×10^{-5}, 2×10^{-5} and 5×10^{-6} kg/m^2/s, and the critical shear stresses are 0.1, 0.2, and 0.5 N/m^2, respectively. Horizontal and vertical diffusion coefficients were set to 0.1 and 0.001 m^2/s. The suspended sediment concentration at the respective boundaries were set to 0.05, 0.04, 0.04, 0.05, and 0.001 kg/m^3. The wind field was derived from the ERA5 reanalysis data with a resolution of $0.25°\times0.25°$, while the wave inputs daily observations from the Dawanshan coastal station. Data on flow velocity and suspended sediment concentration at Stations A2 and A14 were used for model calibration. Model performance was subsequently evaluated using the RMSE, SS, and r metrics. The results indicate that the model effectively reproduces the hydrodynamic and suspend sediment variation characteristics within the study area. (Figure 2-4).

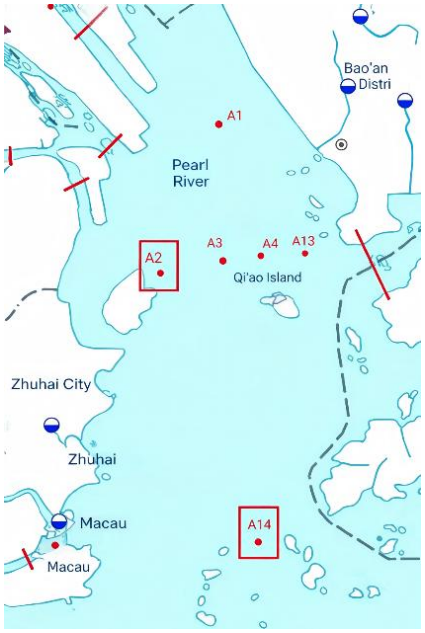


Figure 2. Site locations

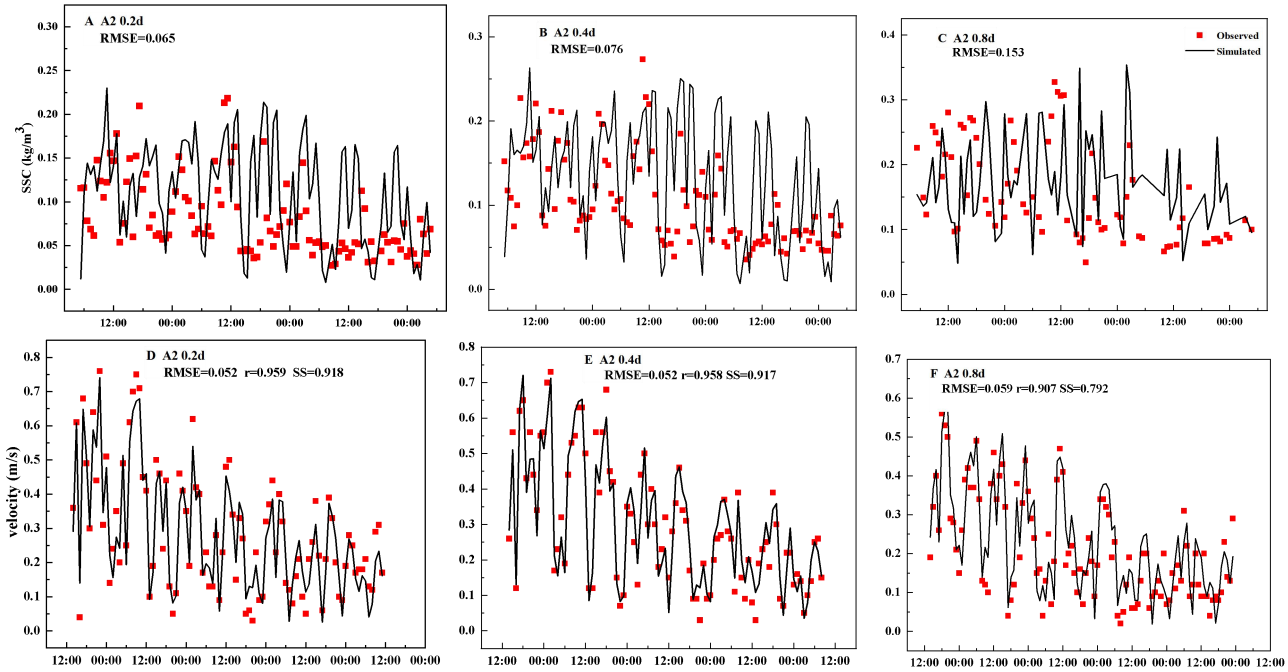


Figure 3. Validation of SSC (A-C), velocity (D-F) at Station A2 in surface/middle/bottom layers

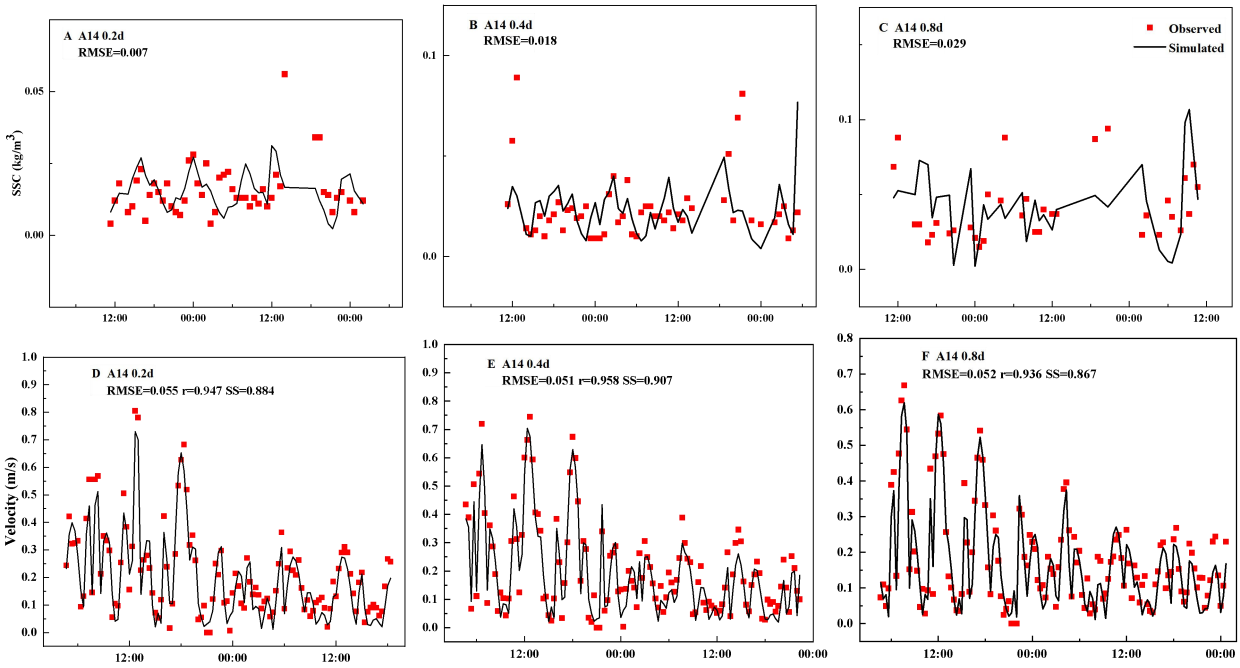


Figure 4. Validation of SSC (A-C), velocity (D-F) at Station A14 in surface/middle/bottom layers

4. IMPACT OF WIND FARM DISTURBANCES ON HYDRO-SEDIMENT DYNAMICS

The simulation period is from July 20 to August 5, 2015. Model boundary conditions, wave fields, and wind forcing were derived from data within this specific period, while all other parameters setting remained consistent with the calibration phase.

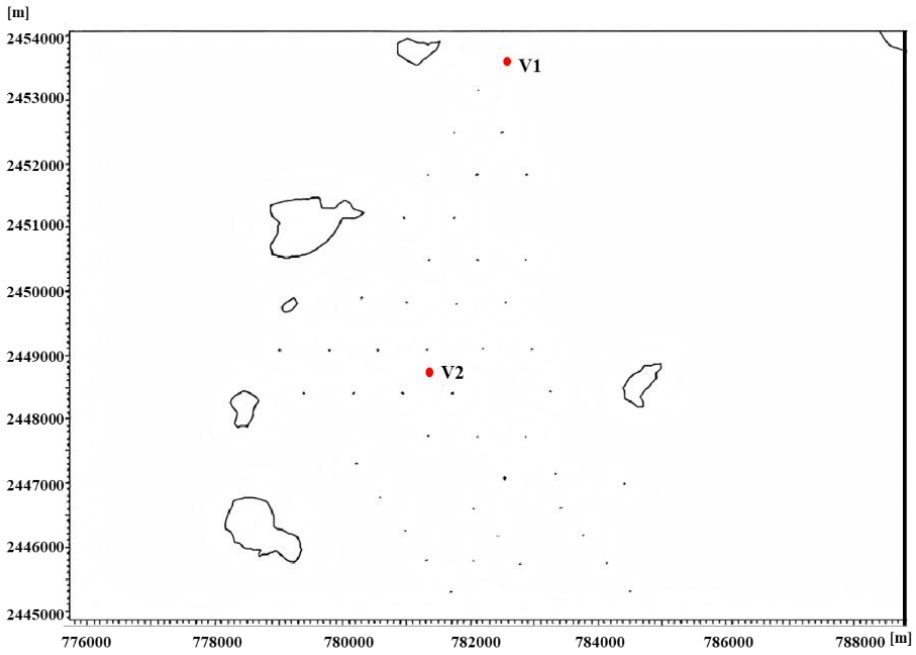


Figure 5. Schematic of the selected observation stations

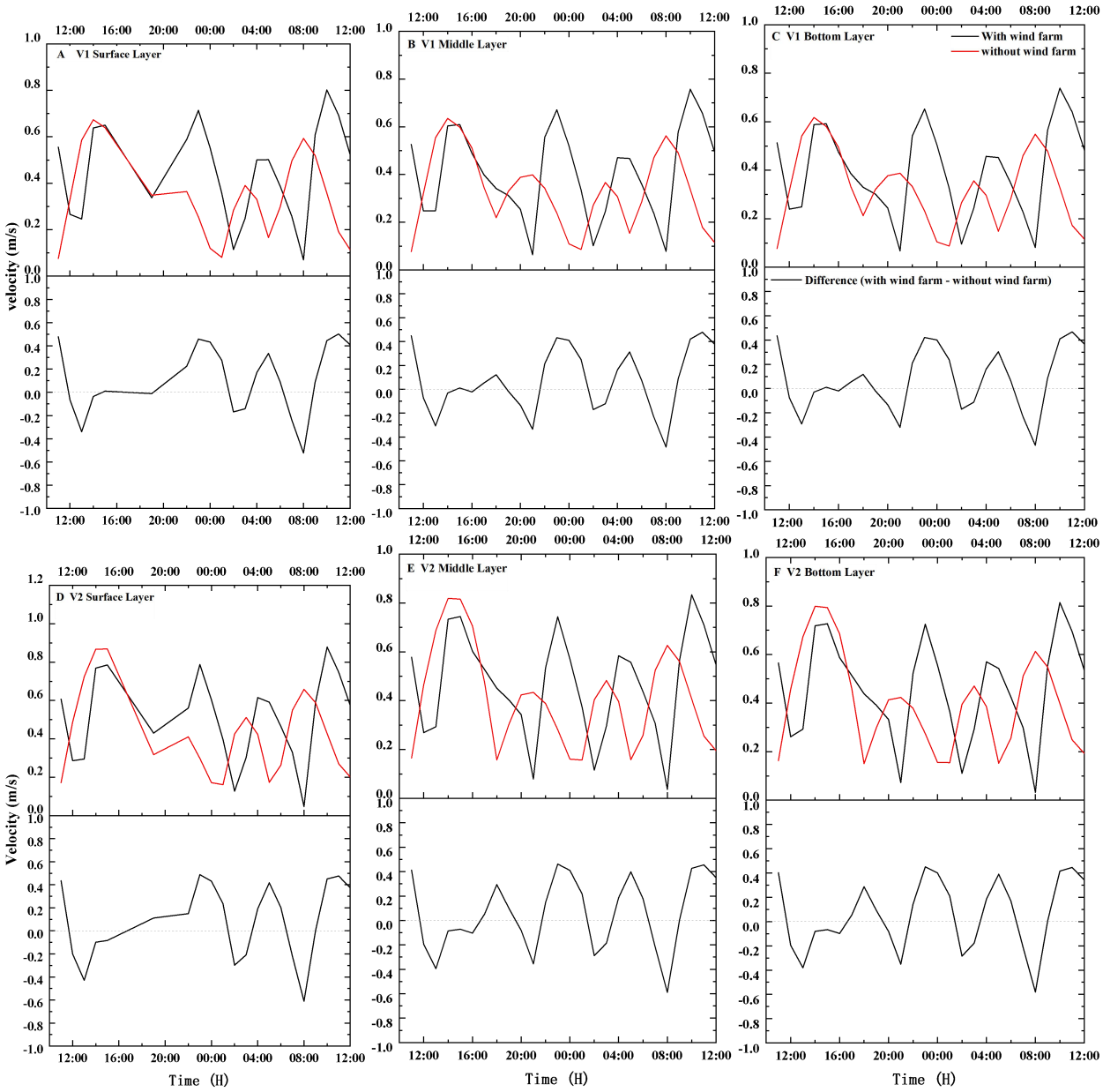


Figure 6. Comparison of vertical velocity profiles with and without the offshore wind farm

All the stations are shown in Figure 5. The Station V1 has vertical response characteristics. The velocity differences at Station V1 are generally between -0.55 and 0.50 m/s as you can see in Figure 6. At the surface of Station V1, the maximum and minimum differences are 0.502 and -0.523 m/s. In the layer of Station V1 these differences are 0.478 and -0.484 m/s. At the bottom of Station V1 the differences are about meters per second.

The hydrodynamic perturbations at Station V1 happen. This movement creates a kind of acceleration belt due to the Venturi effect, which is caused by the flow contraction. On the hand Station V2 is located at the northern boundary of the array. The velocity deviations across the water column at Station V2 range from 0.45 m/s to -0.61 m/s. The middle and bottom layers of Station V2 experience the intense deceleration.

These vertical profiles at Station V1 and Station V2 are very interesting at 23:00 and 08:00. They show that the wake-induced disturbances in the layers of Station V1 and Station V2 are very strong and consistent but the surface responses are more unpredictable. The Station V1 and Station V2 behave differently due, to their locations and the hydrodynamic perturbations they experience.

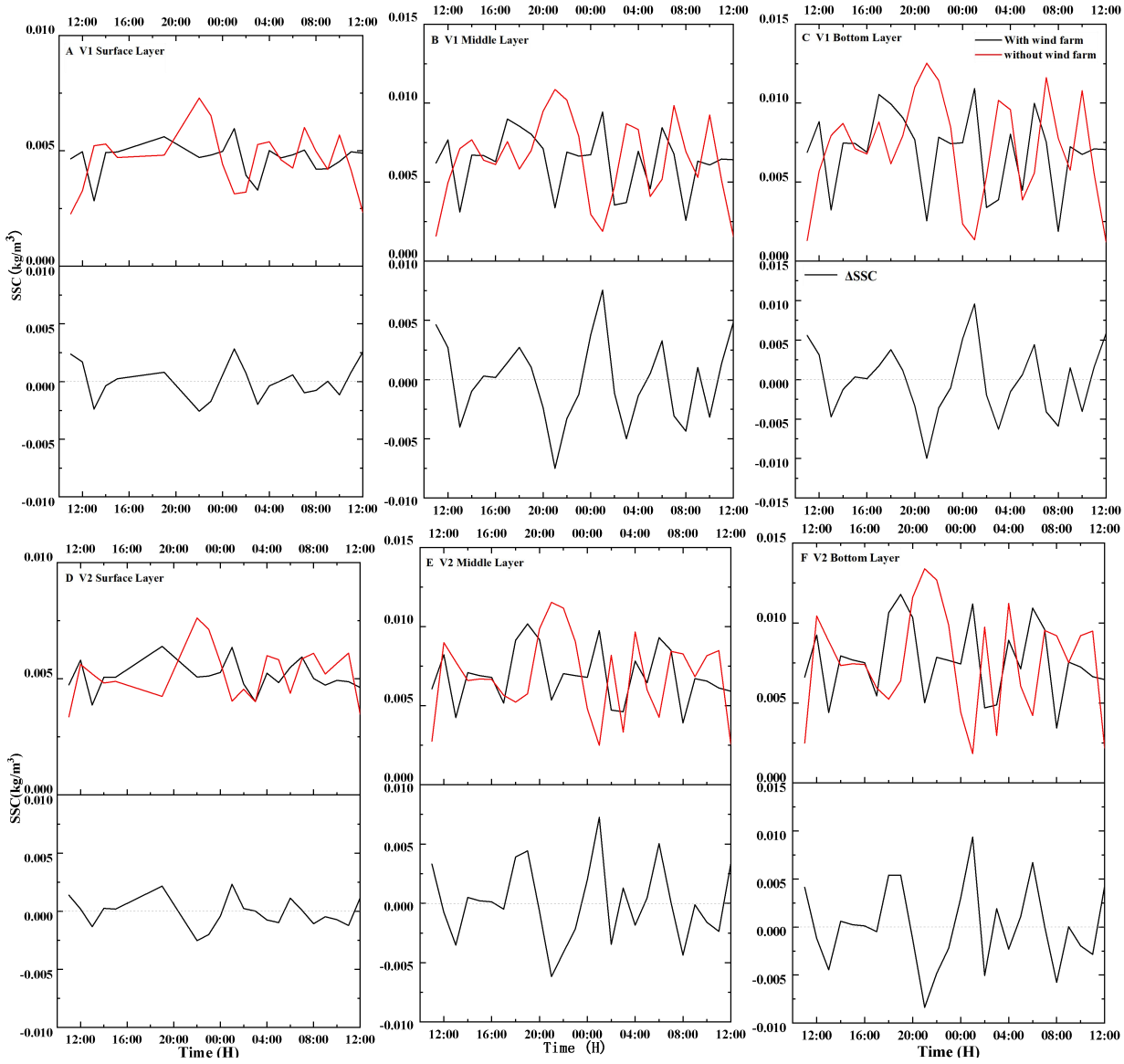


Figure 7. Comparison of vertical SSC profiles with and without the offshore wind farm

As shown in Figure 7, station V1 have only small ΔSSC values—mostly around zero, within 10^{-3} to 10^{-2} kg/m³. Station V2, in contrast, has a clear negative bias, and the disturbance grows with depth. By 8:00 the next day, negative anomalies cover most of the study area. A continuous low- value belt appears in the middle and bottom layers. At the surface, positive increments (0.002–0.005 kg/m³) show up only at the outer edges or inside isolated channels. This indicates that the impact of the wind farm on suspended sediment concentration is mainly concentrated at the bottom layer and shows a vertical distribution pattern. The changes in suspended sediment concentration vary in different water layers. However, as the water depth increases, the changes gradually become larger.

5. CONCLUSIONS

In this study, the 3D model is used to describe the coupling relationship between hydrodynamics and sediment, and the field data are collected. The main conclusions are as follows:

(1) The flow velocity in the study area changes significantly, but the difference between different water layers is not obvious, only about 0.1 m/s.The flow velocity increases sharply between the channels, and the flow velocity decreases at the edge of the wind farm.

(2) The suspended sediment concentration is a concept that exists at the bottom, and its changes will be more and more significant with the increase of water depth, generally within 0.001-0.01 kg/m³.The construction of wind farms will have a negative impact on the seabed flow structure, which is not conducive to the deposition of sediment.

ACKNOWLEDGEMENTS

This research was financially supported by the Southern Marine Science and Engineering Guangdong Laboratory (Zhuhai) (No. SML2024SP024).

REFERENCES

[1] Qi, W. G., and Gao, F. P., "Physical modeling of local scour development around a large-diameter monopile in combined waves and current," Coastal Engineering 83, 72-81 (2014).
[2] Sumer, B., and Fredsoe, J., "Scour around Pile in Combined Waves and Current," Journal of Hydraulic Engineering 127(5), 403-411 (2001).
[3] Zanke, U. C. E., Hsu, T. W., Roland, A., *et al.*, "Equilibrium scour depths around piles in noncohesive sediments under currents and waves," Coastal Engineering 58(10), 986-991 (2011).
[4] Murray, A. B., and Paola, C., "A cellular model of braided rivers," Nature 371, 54-57 (1994).
[5] Seminara, G., "Fluvial Sedimentary Patterns," Annual Review of Fluid Mechanics 42, 43-66 (2010).
[6] Coco, Z. G., Townend, I., *et al.*, "Is "Morphodynamic Equilibrium" an oxymoron?," Earth-Science Reviews 165, 257-267 (2017).
[7] Carpenter, J. R., Merckelbach, L., Callies, U. *et al.*, "Potential Impacts of Offshore Wind Farms on North Sea Stratification," PLOS ONE 11(8), 1-28 (2016).
[8] Cazenave, P. W., Torres, R., and Allen, J. I., "Unstructured grid modelling of offshore wind farm impacts on seasonally stratified shelf seas," Progress in Oceanography 145, 25-41 (2016).
[9] Garrett, C., and Cummins, P., "The efficiency of a turbine in a tidal channel," Journal of Fluid Mechanics 588, 243-251 (2007).
[10] Christiansen, M. B., and Hasager, C. B., "Wake effects of large offshore wind farms identified from satellite SAR," Remote Sensing of Environment 98(2), 251-268 (2005).
[11] Li, X., Chi, L., Chen, X., *et al.*, "SAR observation and numerical modeling of tidal current wakes at the East China Sea offshore wind farm," Journal of Geophysical Research: Oceans 119, 4958-4971 (2014).
[12] Hosseini, S. T., Pein, J., Staneva, J., *et al.*, "Impact of offshore wind farm monopiles on hydrodynamics interacting with wind-driven waves," Ocean Modelling 195, 102521 (2025).
[13] Vanhellemont, Q., and Ruddick, K., "Turbid wakes associated with offshore wind turbines observed with Landsat 8," Remote Sensing of Environment 145, 105-115 (2014).
[14] Vanhellemont, Q., "Adaptation of the dark spectrum fitting atmospheric correction for aquatic applications of the Landsat and Sentinel-2 archives," Remote Sensing of Environment 225, 175-192 (2019).
[15] Rivier, A., Bennis, A. C., Pinon, G., *et al.*, "Parameterization of wind turbine impacts on hydrodynamics and sediment transport," Ocean Dynamics 66(10), 1285-1299 (2016).